Black Sea Journal of Engineering and Science
doi: 10.34248/bsengineering.1863508

Open Access Journal
e-ISSN: 2619 – 8991

Research Article
Volume 9 - Issue 2: 812-825 / March 2026

LIQUEFACTION, BUILDING RESPONSE, AND SEISMIC SETTLEMENT MECHANISMS IN THE ADAPAZARI BASIN

Davut YILMAZ[1]*

[1]*Ankara Yıldırım Beyazıt University, Department of Civil Engineering, 06010, Ankara, Türkiye*

Abstract: The 17 August 1999 Mw 7.4 Kocaeli earthquake caused widespread settlement of buildings in downtown Adapazarı, although clear surface evidence of free-field liquefaction was limited. This study investigates the mechanisms responsible for these settlements by integrating nonlinear site response analysis, liquefaction assessment, and foundation-level deformation modeling. Because the main shock was not recorded in the city center, ground motions were estimated using nonlinear site response analyses performed with the D-MOD program and calibrated against recorded aftershocks. The resulting peak ground acceleration in downtown Adapazarı was estimated to be approximately 0.30 g. Simplified free-field liquefaction analyses predicted liquefaction in shallow silty and sandy silt layers between depths of 1.5 m and 4.0 m. However, strain restriction enforced by a stiffer surrounding soil matrix, which restricted the formation of shear strain in potentially liquefiable strata, is responsible for the lack of broad free-field manifestations. Localized liquefaction beneath shallow foundations resulted from structural reaction effects that greatly increased cycle stress ratios beneath buildings, especially for short-period structures. Liquefaction-induced volumetric strains account for approximately 40–50% of the observed settlements. The remaining settlement is explained by lateral sliding of supporting soils once seismic bearing capacity was exceeded, as evaluated using simplified Newmark-type sliding block analyses. The findings demonstrate that building settlements in Adapazarı resulted from the combined effects of soil stratigraphy, structural response, and foundation-level deformation, highlighting the limitations of free-field liquefaction procedures for urban settings.

Keywords: Nonlinear site response analysis, Liquefaction-induced settlement, Seismic settlement

***Corresponding author:** Ankara Yıldırım Beyazıt University, Department of Civil Engineering, 06010, Ankara, Türkiye
E mail: yilmazdavut1967@gmail.com (D. YILMAZ)
Davut YILMAZ https://orcid.org/0000-0002-9981-7875

Received: January 14, 2026
Accepted: February 18, 2026
Published: March 15, 2026

Cite as: Yılmaz, D. (2026). Liquefaction, building response, and seismic settlement mechanisms in the Adapazarı basin. *Black Sea Journal of Engineering and Science*, *9*(2), 812-825.

1. Introduction

Liquefaction is the transformation of a granular soil from a solid to a fluid-like state caused by increased pore-water pressure and the consequent reduction in effective stress (Marcuson, 1978). Excess pore pressure develops as granular soils contract under cyclic shear loading. This phenomenon occurs most readily in loose to moderately dense, poorly drained soils such as silty sands or sands interbedded with low-permeability layers, resulting in soil softening and large cyclic strains.

Following the 1964 Alaska and Niigata earthquakes, Seed and Idriss (1971) introduced the simplified procedure for evaluating liquefaction potential. The method was subsequently refined by Seed (1979), Seed and Idriss (1982), and Seed et al. (1985). Workshops organized in 1985 (NRC, 1985) and 1996 (Youd and Idriss, 1997) further advanced the methodology, culminating in the revised procedure presented by Youd and Idriss (2001), which is adopted in this study.

The procedure is empirically based on field case histories and laboratory data, primarily from level to gently sloping sites underlain by shallow (<15 m) Holocene alluvial or fluvial deposits. Its applicability is therefore generally limited to similar site conditions.

Earthquake-induced liquefaction and associated ground deformations continue to be a major cause of damage to buildings and infrastructure in urban areas underlain by young alluvial deposits. While simplified liquefaction evaluation procedures have been widely adopted in engineering practice, post-earthquake observations repeatedly demonstrate that structural damage and settlement patterns cannot always be explained by free-field liquefaction analyses alone. In many cases, significant settlements occur beneath buildings despite limited evidence of liquefaction at the ground surface, highlighting the importance of soil–structure interaction and foundation-level deformation mechanisms.

The 17 August 1999 Mw 7.4 Kocaeli earthquake provides a compelling example of this discrepancy. In downtown Adapazarı, widespread settlements of shallow-founded buildings were observed, yet clear surface manifestations of free-field liquefaction were sparse. Numerous post-earthquake investigations (Bray et al., 2001; Sancio et al., 2002) documented substantial building settlements and tilting, particularly in areas underlain by shallow silty and sandy silt deposits, raising questions regarding the

adequacy of conventional liquefaction assessment methods for explaining the observed damage patterns.

Previous studies have shown that the seismic response of deep alluvial basins may significantly modify ground motions through basin amplification and prolonged shaking (Bard and Bouchon, 1985; Rial et al., 1992). In addition, the presence of structures alters stress conditions within the underlying soil, potentially increasing cyclic stresses beneath foundations while simultaneously suppressing liquefaction in adjacent free-field areas. These effects are not captured by traditional level-ground liquefaction procedures, which assume horizontally layered deposits and neglect building response.

The objective of this study is to investigate the mechanisms governing building settlements in downtown Adapazarı by integrating nonlinear site response analysis, liquefaction assessment, and foundation-level deformation modeling. Because the main shock was not recorded in the city center, ground motions are first estimated using nonlinear site response analyses calibrated with recorded aftershocks. Liquefaction potential is then evaluated for both free-field conditions and beneath buildings, accounting for the effects of soil stratigraphy and structural response. Finally, settlement mechanisms are examined by combining estimates of liquefaction-induced volumetric strain with lateral soil movement beneath foundations using simplified seismic bearing-capacity and sliding block concepts.

By linking observed building performance with site-specific ground motions and foundation-level deformation mechanisms, this study provides a physically consistent explanation for the settlement patterns observed in Adapazarı. The findings highlight the limitations of free-field liquefaction procedures for urban environments and underscore the need to incorporate simplified soil–structure interaction and seismic bearing-capacity effects in post-earthquake damage assessment and engineering practice.

2. Materials and Methods

The main objective of this study is to identify the key factors influencing structural settlements. For this purpose, the estimation of earthquake ground acceleration in the Adapazarı city center is first carried out. In the subsequent section, the effects of structures on liquefactions are examined. Finally, the mechanism of structural settlement is analyzed, and the calculated displacement values are compared with field observations.

2.1. The estimation of earthquake ground acceleration in the Adapazarı city center for 17 August 1999 Earthquake.

2.1.1. Characteristics of the Adapazarı basin and ground motion measurements

2.1.1.1. Basin characteristics

The 17 August earthquake caused surface ruptures along the Gölcük, Sapanca, Sakarya, and Karadere segments of the North Anatolian Fault. The Sakarya segment runs along the immediate boundary of the Adapazarı Basin. The Adapazarı Basin is an ancient lakebed, where lacustrine deposits are overlain by alluvial sediments transported by the Sakarya River and Çark Stream.

A 200 m–deep borehole drilled in the city center of Adapazarı by the General Directorate of State Hydraulic Works (DSİ) revealed that the thickness of the alluvial deposits is approximately 40 m, and that the bedrock lies at depths greater than 200 m.

Owing to the meandering river regime and the accompanying sedimentation processes, the soil properties within the upper 40 m show pronounced variability in both vertical and lateral directions (Sancio et al., 2002). However, softer inclusions generally exert a limited effect, as the overall deformation response is dominated by the surrounding stiffer matrix. Consequently, the stresses developed within these softer inclusions are lower than those in the stiffer matrix and also lower than the values estimated using conventional analysis methods (Pyke, 2003 and 2004). The emphasis articulated by him provided the basis for selecting an appropriate shear-wave velocity profile for the site response analysis and for defining the depth-dependent SPT and CPT profiles used in the liquefaction assessment.

Through a collaborative effort involving the University of California, Berkeley, the University of California, Los Angeles, Brigham Young University, Sakarya University, ZETAŞ Corporation, Middle East Technical University, and Boğaziçi University, a comprehensive field investigation program was carried out to evaluate soil conditions at sites affected by ground failure across Adapazarı (Bray et al., 2001). As part of this program, shear-wave velocity measurements were obtained using seismic cone penetration testing techniques (Durgunoğlu et al., 2000). Figure 1 illustrates the depth-dependent variation of shear-wave velocity at the different test locations.

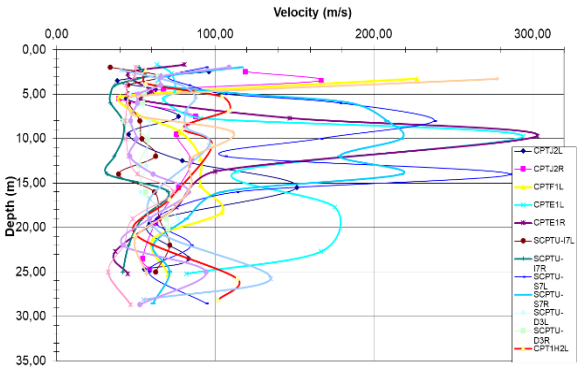

Figure 1. Shear wave velocity profile from seismic cone penetration tests.

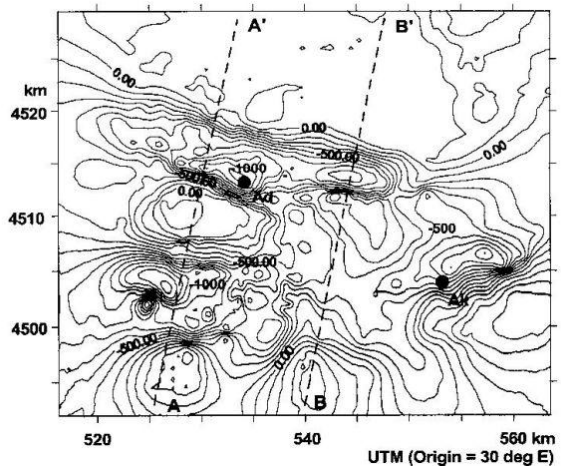

Figure 2. The depth to bedrock (Komazawa et al., 2002).

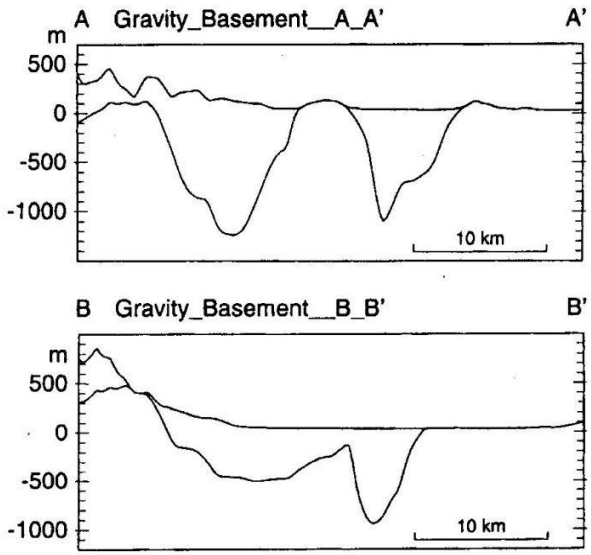

Figure 3. Cross sections (Komazawa et al., 2002).

2.1.1.2. Ground Motion Measurements at the Site

The SKR strong-motion station, located approximately 3 km from the city center of Adapazarı, is situated on soft rock at the margin of the Adapazarı Basin. During the 1999 Kocaeli earthquake (Mw = 7.4), the station recorded acceleration time histories only in the east–west (fault-parallel) direction (Figure 4).

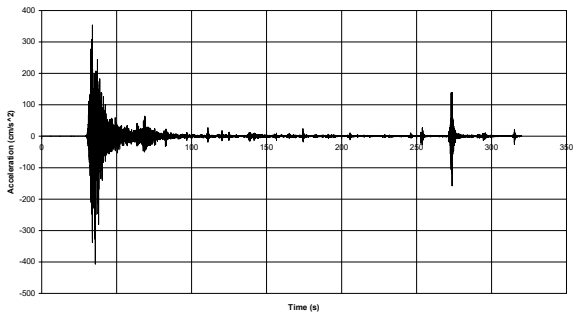

Figure 4. Recorded main shock at the SKR station August 17, 1999, Earthquake.

The IMAR aftershock station, co-located with SKR, and the HAST station, installed on soft soil in the downtown area of Adapazarı, recorded acceleration time histories during the 13 September aftershock (M = 5.8) (Figures 5 a–d).

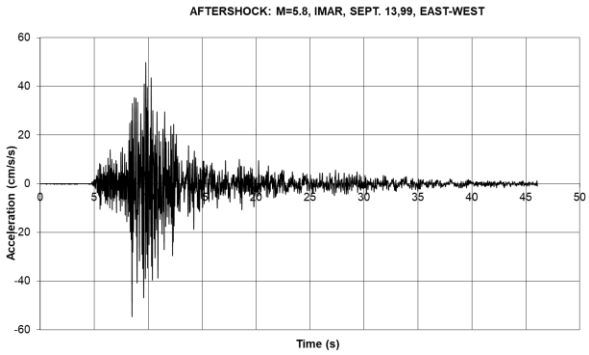

(a)

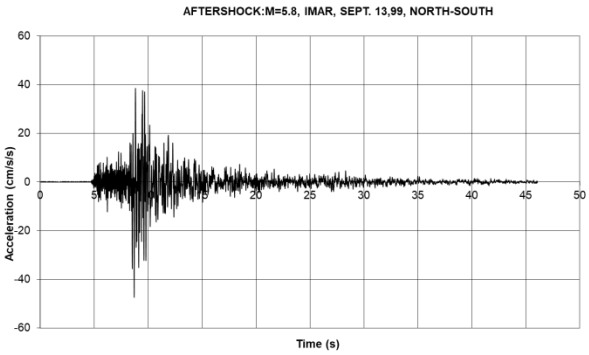

(b)

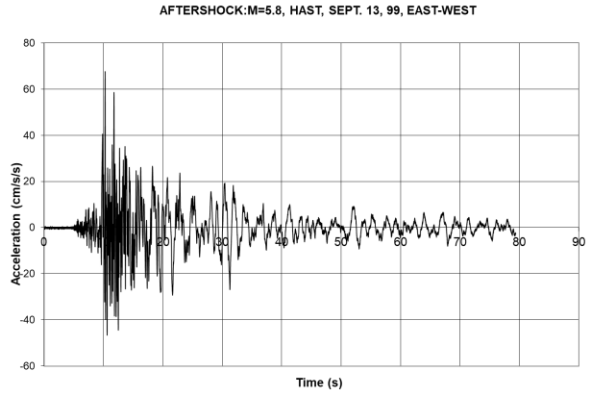

(c)

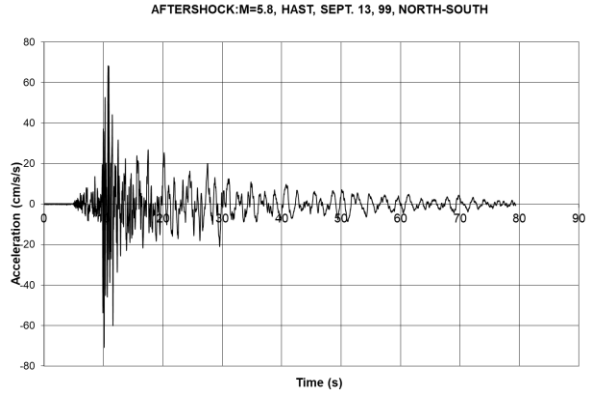

(d)

Figure 5. Acceleration time histories recorded at the aftershock stations IMAR and HAST.

2.1.2. Nonlinear site response modeling framework

2.1.2.1. Nonlinear hyperbolic constitutive model

Under drained or undrained loading conditions, the initial shear stress–strain response of soils is commonly represented by a hyperbolic constitutive model. Assuming a hyperbolic relationship between shear stress τ and shear strain γ, the constitutive (equation 1) is given by:

$$\tau = f(\gamma) = \frac{G_{mo}\,\gamma}{1+\beta\left(\frac{G_{mo}}{\tau_{mo}}\gamma\right)^{s}} = \frac{G_{mo}}{1+\beta\left(\frac{\gamma}{\gamma_r}\right)^{s}} \quad (1)$$

where $G_{mo}$is the small-strain shear modulus, $\tau_{mo}$is the shear stress corresponding to approximately 1% shear strain, and $\gamma_r = \tau_{mo}/G_{mo}$is the reference shear strain (Hashash and Park, 2001). The parameters $\beta$and $s$define the degree of nonlinearity of the shear stress–shear strain (τ–γ) relationship. This formulation is consistent with constitutive models adopted in SHAKE-type equivalent-linear analyses and nonlinear implementations such as D-MOD.

2.1.2.2. One-Dimensional wave propagation and damping formulation

Free-field site response is modeled assuming vertically propagating one-dimensional shear waves, which account for approximately 75% of seismic energy transmission (Kramer, 1996). The soil profile is discretized into nhorizontal layers and represented using a lumped-mass model, where each layer consists of a mass connected by nonlinear springs and viscous dashpots, with stiffness degrading as a function of shear strain.

Motion (equation 2) in matrix form is:

$$[M]\{\ddot{u}\} + [C]\{\dot{u}\} + [K]\{u\} = -[M]\{I\}\ddot{u}_g \quad (2)$$

where [M], [C], and [K]denote the mass, damping, and stiffness matrices; {u}, {u̇}, and {ü} are displacement, velocity, and acceleration vectors; and $\ddot{u}_g$is the prescribed base acceleration. The mass of the i-th (equation 3) layer is:

$$m_i = \rho_i h_i \quad (3)$$

At shear strain levels below approximately 10^{-4}–10^{-2}, the hyperbolic model behaves nearly linearly and produces negligible hysteretic damping. To avoid unrealistically high response amplitudes, Rayleigh damping is introduced (equation 4), consistent with D-MOD implementations (Matasovic, 1993; Hashash and Park, 2001):

$$[C] = \alpha_R[M] + \beta_R[K] \quad (4)$$

Because the mass-proportional damping coefficient α_R is much smaller than the stiffness-proportional term, the damping matrix (equation 5) can be simplified as:

$$[C] = \beta_R[K] \quad (5)$$

The stiffness-proportional damping coefficient $\beta_R$is obtained from the target viscous damping ratio ξ associated with the first vibration mode (equation 6):

$$\xi = \frac{\beta_R \pi}{T_1} \quad (6)$$

where the fundamental period T_1 (equation 7) is estimated as:

$$T_1 = \frac{4H}{V_s} \quad (7)$$

with H denoting the soil column height and V_s the shear-wave velocity.

Previous studies (Hudson et al., 1994; Hashash and Park, 2001) have shown that for soil columns exceeding 100 m in height, frequency-dependent damping in the time domain becomes increasingly important. Accordingly, the Rayleigh coefficients are selected using two representative circular frequencies $\omega_m$and ω_n (equation 8):

$$\alpha_R = 2\xi\frac{\omega_m\omega_n}{\omega_m+\omega_n}, \beta_R = 2\xi\frac{1}{\omega_m+\omega_n} \quad (8)$$

The stiffness matrix is updated at each time step based on the strain-dependent shear modulus. For the i-th layer, stiffness is computed as (equation 9):

$$k_i = \frac{G_i}{h_i} = \frac{\Delta\tau_i(\gamma_i)}{h_i\Delta\gamma_i} \quad (9)$$

where $G_i$is the shear modulus corresponding to the current strain level. The shear stress $\Delta\tau_i$is evaluated using the hyperbolic stress–strain relationship.

The elastic half-space underlying the soil column is modeled using a viscous boundary, where the damping coefficient is proportional to the product of soil density and shear-wave velocity (equation 10) (Joyner and Chen, 1975):

$$C_E = \rho V_{se} \quad (10)$$

Here, C_E is the viscous damping coefficient, ρ is the mass density, and V_{se} is the shear-wave velocity of the elastic base. Initially, a stiffness matrix is assumed, and the equation of motion is solved using Newmark's β integration method. Based on the resulting shear strains and stresses, the stiffness matrix is updated, and the equation of motion is solved again. This iterative procedure is repeated until the difference between the computed shear strains and the previously assumed values falls below a prescribed convergence tolerance.

2.1.3. Estimation of ground motion in downtown Adapazarı

2.1.3.1. General

This chapter presents the estimation of the main-shock ground motion of the 17 August 1999 Kocaeli earthquake in downtown Adapazarı using the nonlinear site response program D-MOD, with minor modifications. Because the main shock was not recorded in the city center, aftershock records are used to calibrate the model.

The use of SHAKE (Schnabel et al., 1972) is not considered appropriate due to its depth limitations, which are inadequate for the deep basin conditions of Adapazarı. D-MOD has been successfully applied to deep

soil sites (Chang et al., 1997), solid waste fills (Bray and Rathje, 1998), and back-analyses of well-documented case histories, including Treasure Island during the Loma Prieta earthquake (Matasovic, 1993).

Estimating the main shock is necessary to understand subsurface soil behavior and to draw practical conclusions from the observed performance of foundations and buildings.

Basin curvature may trap body waves and convert them into surface waves, producing stronger shaking and longer durations than predicted by one-dimensional vertically propagating shear-wave analyses (Rial et al., 1992). These effects are implicitly captured through aftershock-based model calibration.

The estimation procedure consists of two steps: (1) model parameters are adjusted to match aftershock recordings on the basin using rock-site motions adjacent to the basin as input; (2) the recorded rock motion is applied to estimate the main-shock ground motion in the basin.

2.1.3.2. IMAR aftershock station co-located with SKR

The SKR strong-motion station, located approximately 3 km from downtown Adapazarı, is situated on soft rock at the basin margin. During the 1999 Kocaeli earthquake (Mw = 7.4), acceleration was recorded only in the east–west (fault-parallel) direction (Figure 4). The IMAR aftershock station, co-located with SKR, and the HAST station, installed on soft soil in downtown Adapazarı, recorded acceleration time histories during the 13 September 1999 aftershock (M = 5.8) (Figures 5 a–d).

2.1.3.3. Analytical soil profile

The basin is filled with lacustrine sediments and alluvium to a depth of approximately 200 m, while total basin depth beneath the city reaches about 1000 m. Detailed logs for the upper 200 m are provided in Yilmaz (2003); no data are available below this depth.

A shear-wave velocity profile (Figure 6) was constructed using available measurements given in Yilmaz (2003), ensuring that the site's predominant period does not exceed that inferred from Figure 3. The viscous damping ratio ζ is taken as 1% at the ground surface and decreases with depth due to increasing confining stress (Hashash and Park, 2001; Figure 7).

The initial shear modulus G_{mo} is computed from the shear-wave velocity profile and a soil density of $\rho = 2\,\mathrm{g/cm^3}$. The shear stress τ_{mo} is derived from modulus reduction curves using the reference-strain approach, resulting in increasing τ_{mo} with depth. Hyperbolic model parameters are taken as $\beta = 1.4$ and $s = 0.8$ (Matasovic, 1993).

Rayleigh damping coefficients are determined by using the first and eighth modes and frequency-dependent damping, with $\zeta(8) = 0.37\zeta$, yielding $\alpha_R = 0.98\zeta$ and $\beta_R = 0.013\zeta$.

The soil column base is modeled as a visco-elastic half-space with $\rho = 2.25\,\mathrm{g/cm^3}$ and $V_{SE} = 3000\,\mathrm{m/s}$. Pore-water pressure generation is neglected; therefore, total-stress analysis is performed.

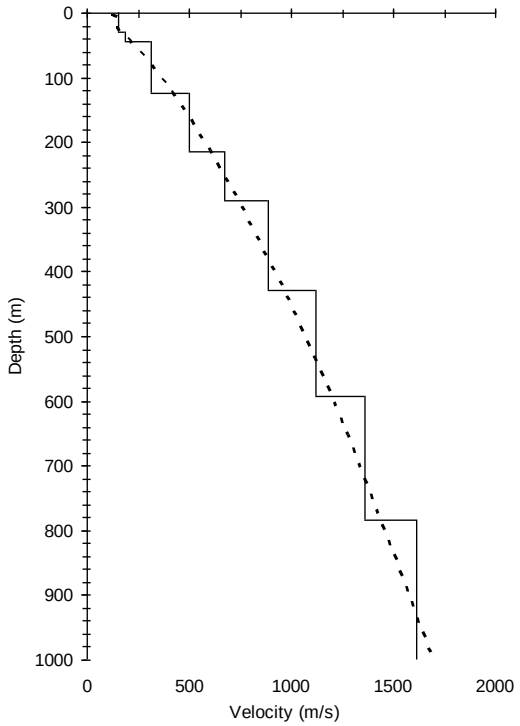

Figure 6. Shear wave velocity profile.

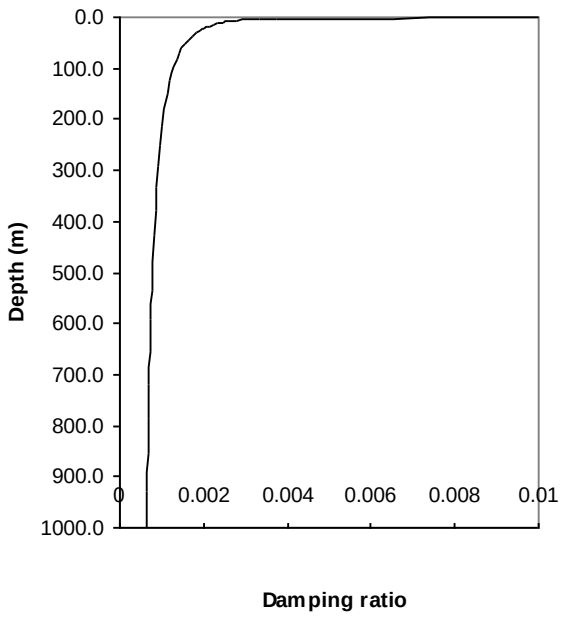

Figure 7. Influence of confining pressure on damping (Hashash and Park, 2001).

2.1.4.4. Analysis

Model calibration is conducted by using IMAR recordings as input and matching computed motions to those recorded at HAST for the 13 September 1999 aftershock. Peak accelerations at IMAR are 0.048 g (north–south) and 0.056 g (east–west), while HAST recorded 0.072 g and 0.068 g, respectively.

Deconvolution of the IMAR and SKR ground motion records was deemed unnecessary as both stations are founded on soft rock consistent with the velocity profile in Figure 8. Model parameters are adjusted to match

peak accelerations at HAST, with emphasis placed on peak values rather than response spectra, which tend to underestimate observed accelerations.

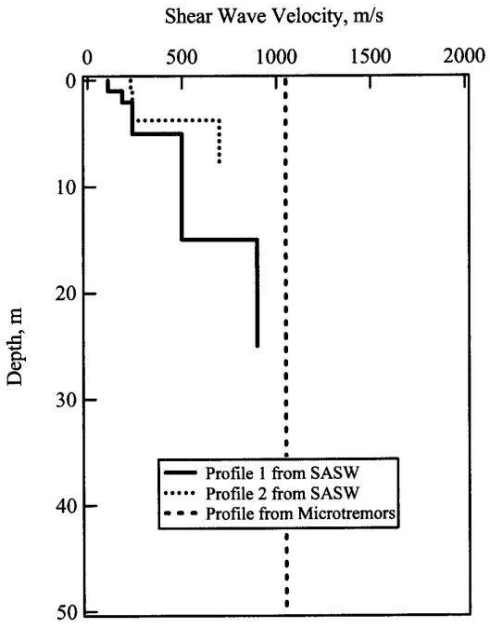

Figure 8. Shear wave velocity profile SKR (Rosenblad et al., 2003).

The model was calibrated such that the computed peak ground accelerations closely matched the recorded values in both horizontal directions at the HAST station. The computed peak acceleration matches the measured value in the north–south direction (0.072 g) and slightly underestimates the east–west component (0.065 g vs. 0.068 g).

In addition, response spectral accelerations were evaluated to further assess the quality of the calibration. Greater emphasis was placed on matching peak accelerations rather than response spectral ordinates, as the latter tended to underestimate the measured accelerations. Figures 9 and 10 present the pseudo-acceleration response spectra derived from the calculated and recorded acceleration time histories at the HAST station.

Following calibration, the main-shock motion in downtown Adapazarı is estimated. The computed east–west time history as shown in Figure 11 yields a peak acceleration of approximately 0.30g.

This estimate agrees with empirical predictions for deep cohesionless soils (~0.30 g), while median relations suggest values up to 0.40 g (Figure 10). Parametric analyses indicate that peak ground acceleration in downtown Adapazarı likely did not exceed 0.35 g during the 17 August 1999 earthquake.

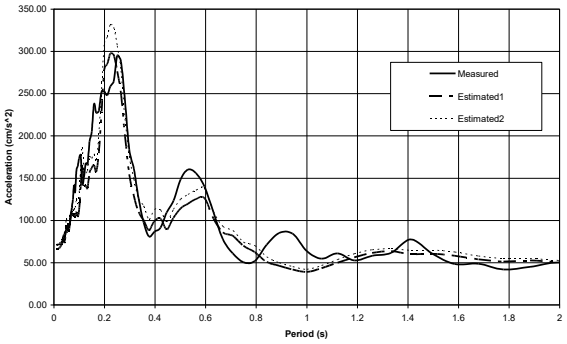

Figure 9. Measured and estimated pseudo acceleration response spectra in north-south direction. Estimated1 has base density of ρ=2 g/cm^3 and estimated2 has base density of ρ=2.5 g/cm^3.

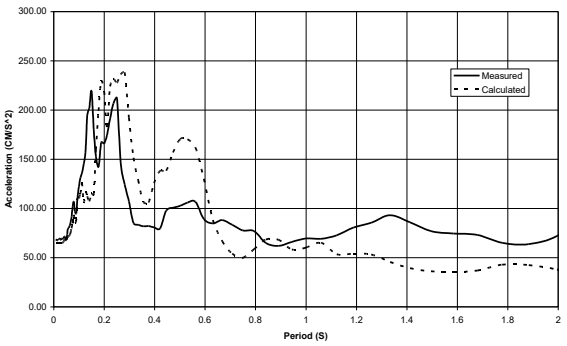

Figure 10. Measured and estimated pseudo acceleration response spectra in east-west direction.

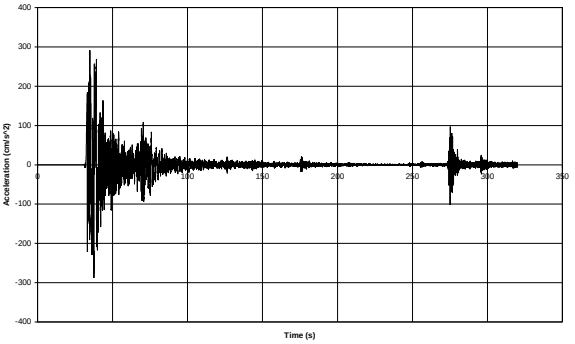

Figure 11. Estimated east-west time history at the downtown from the time history measured at SKR station during August 17, 1999 Earthquake.

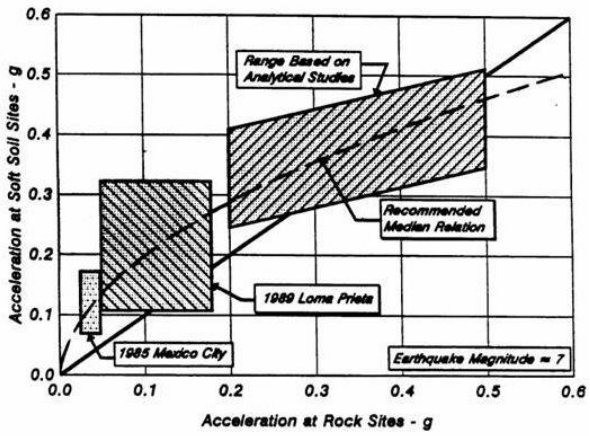

Figure 12. Variations of peak horizontal accelerations at soft soil sites with accelerations at rock sites (Idriss, 1991).

2.2. The Effects of Structures on Liquefactions

2.2.1. General

Post-earthquake field investigations conducted in 2000 documented significant settlements of buildings in downtown Adapazarı, predominantly affecting structures founded on shallow mat foundations without basements (EERI, 2000). Settlements were largely vertical, with some lateral movements observed. The absence of soil bulging around many buildings indicates that settlements commonly occurred without bearing capacity failure and were primarily associated with liquefaction-induced volumetric strains.

Liquefaction potential is evaluated using standard free-field, level-ground procedures, in which the cyclic stress ratio (CSR) induced by earthquake shaking is compared with the cyclic resistance ratio (CRR) derived from SPT- and CPT-based correlations (Seed and Idriss, 1971; Youd and Idriss, 2001). Although this approach neglects soil–structure interaction effects, it is widely adopted due to the lack of robust alternatives and is generally considered conservative (Rollins and Seed, 1990).

For soils beneath structures, additional factors influencing liquefaction response were examined, including increased confining pressure, initial static shear stresses, and building response effects. While increased vertical effective stress beneath buildings tends to reduce CSR, the dynamic response of the structure may either amplify or reduce cyclic stresses depending on the relationship between spectral acceleration and peak ground acceleration.

2.2.2. Effect of building response

In practice, buildings exhibit flexibility and possess a fundamental vibration period. The base shear force developed in a structure is related to the earthquake response spectrum and the building's fundamental period (Newmark and Hall, 1982). The maximum base shear force (equation 11) may be expressed as:

$$V_{\max} \approx 0.8 \frac{S_a}{g} W \tag{11}$$

where $S_a$is the spectral acceleration at the building period and $W$is the building weight (Rollins and Seed, 1990).

The corresponding maximum base shear stress per unit building width B (equation 12) is:

$$\tau_{\max} \approx 0.8 \frac{S_a}{g} \frac{W}{B} \tag{12}$$

Assuming an equivalent uniform cyclic shear stress induced by earthquake shaking (equation 13):

$$\tau_{\text{av}} \approx 0.65 \tau_{\max} \tag{13}$$

and noting that the average effective normal stress at the base of the building (equation 14) is:

$$\sigma_o' = \frac{W}{B} \tag{14}$$

the induced cyclic stress ratio beneath the building (equation 15) can be written as:

$$\left(\frac{\tau_{\text{av}}}{\sigma_o'}\right)_{d\text{-base}} \approx 0.52 \frac{S_a}{g} \tag{15}$$

At the same depth in the free field, the induced cyclic stress ratio (equation 16) is expressed as:

$$\left(\frac{\tau_{\text{av}}}{\sigma_o'}\right)_{d\text{-ff}} \approx 0.65 \frac{a_{\max}}{g} \tag{16}$$

assuming groundwater levels near the foundation level.

Equating Eqs. (15) and (16) yields the condition (equation 17):

$$\frac{S_a}{a_{\max}} \approx 1.25 \tag{17}$$

Thus, when $S_a/a_{\max} > 1.25$, the induced CSR beneath the building exceeds that in the free field; otherwise, CSR beneath the building is reduced, resulting in a lower liquefaction potential.

2.2.3. Interpretation and implications

These results indicate that free-field liquefaction analysis alone may not adequately represent conditions beneath buildings. When spectral amplification at the building's fundamental period is significant, cyclic stresses beneath the structure may exceed free-field values, potentially increasing liquefaction susceptibility. Conversely, for buildings with shorter periods or limited spectral amplification, liquefaction potential beneath the structure is reduced. This mechanism explains part of the observed variability in settlement performance among buildings in downtown Adapazarı.

Overall, the analyses indicate that liquefaction-induced volumetric strains account for approximately 40–50% of the measured building settlements. The remaining settlements are attributed primarily to lateral soil movements beneath foundations, evaluated using simplified Coulomb-type wedge analyses driven by ground motions obtained from nonlinear site response analyses. These findings highlight the importance of incorporating simplified soil–structure interaction effects when interpreting post-earthquake building performance in liquefiable soils.

2.2.4. Combined influence of factors for buildings in Adapazarı

In addition to the factors considered in free-field liquefaction analyses, several building-related effects—including increased confining pressure, initial static shear stresses, changes in vertical effective stress, and structural response—must be considered when evaluating liquefaction potential beneath buildings in Adapazarı.

The building stock affected during the 17 August 1999 earthquake primarily consisted of three- to six-story low-rise structures with short fundamental periods (0.3–0.6 s). These buildings are estimated to impose foundation pressures of approximately 6–12 tons/m^2.

Subsurface investigations indicate that, for soil types 1 and 2, liquefiable loose non-plastic silts and sandy silts occur at shallow depths, beginning at approximately 1.5 m and extending to about 4 m, placing liquefiable layers directly beneath building foundations (Figure 13). Corrected penetration resistance values $(N_1)_{60}$typically range from 3 to 15, with most values between 7 and 10. Fines content commonly exceeds 75%, with liquid limits of 25–35%, and natural water contents generally greater than 0.9 LL (Sancio et al., 2002).

The relative state parameter index ξ_r, which quantifies the difference between the in-situ soil state and the critical state under the same effective stress conditions (Boulanger, 2003), is estimated to range from −0.2 to −0.3, indicating that the soils are denser than the critical state and therefore exhibit reduced contractive behavior and lower free-field liquefaction susceptibility. For this range and an initial static shear stress ratio $\alpha = 0.2$–0.3, the static shear correction factor $K_\alpha$is approximately 0.85–0.90, corresponding to a 10–15% reduction in liquefaction resistance.

The groundwater table is shallow (≈ 1.5 m), coinciding with the base of most foundations. As a result of foundation loading, vertical stresses at depths near 2 m increase from approximately 3 tons/m^2 to 9–15 tons/m^2, leading to an additional 10–15% reduction in cyclic resistance. While this increase in vertical effective stress has little effect on reducing the induced cyclic stress ratio (CSR) immediately beneath foundations, it produces an approximately 20% reduction in CSR at depths of about 4 m.

Normalized response spectra for the estimated east–west (fault-parallel) ground motion indicate a maximum spectral amplification ratio of approximately 2.7. This value exceeds the threshold ratio of 1.25, beyond which building response amplifies the induced CSR beneath structures. Consequently, structural response plays a significant role in increasing cyclic stresses beneath foundations, particularly for short-period buildings.

When all contributing factors are combined, the liquefaction resistance of soils immediately beneath buildings is reduced by approximately 20–30% relative to free-field conditions. At depths of 4–5 m, this reduction is largely offset by decreased CSR due to increased vertical effective stress. However, compared with free-field conditions, the dynamic response of buildings results in an increase in induced CSR of up to approximately 100%, when an average spectral amplification ratio of 2.5 is considered.

2.2.5. Liquefaction and settlement assessment in downtown Adapazarı

Liquefaction potential was evaluated for soils extending between depths of 1.5 m and 4.0 m (soil types 1 and 2; see Figure 13). Under free-field conditions and a peak ground acceleration of $a_{\max} = 0.3g$, the cyclic stress ratio (CSR) was calculated as approximately 0.20, while the corresponding cyclic resistance ratio (CRR) was estimated as 0.18 for $(N_1)_{60} = 10$. These values indicate that liquefaction would be expected to occur. However, no clear surface manifestations of liquefaction were observed in free-field areas of Adapazarı, suggesting that the simplified procedure may be overly conservative for the prevailing subsurface conditions.

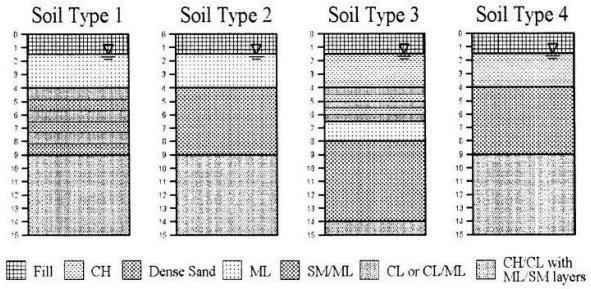

Figure 13. Generalized subsurface conditions in downtown Adapazarı.

As emphasized by Pyke (2003), the simplified liquefaction procedure assumes horizontally stratified soil deposits. In Adapazarı, potentially liquefiable silts and sandy silts are frequently embedded within or underlain by stiffer sand or clayey sand layers. In such composite deposits, shear strains within the liquefiable layers are governed by the deformation of the surrounding stiffer matrix, resulting in lower stress and strain levels than those predicted by free-field simplified methods. This interpretation is supported by shear strain time histories (Figure 14), which show a maximum shear strain of approximately 1.7%.

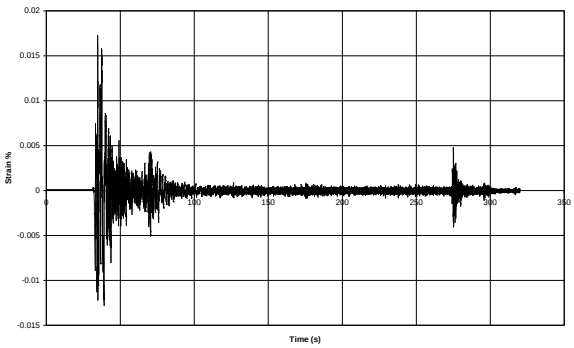

Figure 14. Shear strain time history on the surface of Adapazarı.

Experimental evidence indicates that cyclic softening or initial liquefaction associated with full excess pore-water pressure buildup typically corresponds to shear strains on the order of 2–3% (Ishihara, 1993). The reduced strain levels observed in Adapazarı therefore provide a plausible explanation of building effect on liquefaction in the absence of free-field liquefaction.

Beneath buildings, the calculated CSR increases to approximately 0.40, while the corresponding CRR remains close to 0.15. According to Youd and Idriss (2001), liquefaction may occur even at ground accelerations substantially lower than 0.3g under such conditions. Building response effects are expected to increase shear strains beneath foundations relative to free-field conditions.

Because foundation embedment depths are generally less than 1.5 m, the passive resistance of the surrounding soil is limited. During the earthquake, inertial forces transmitted from the superstructure to the foundation likely exceeded the available shear strength at the foundation–soil interface. Consequently, some buildings experienced plastic sliding or rocking, generating localized shear strains sufficient to trigger liquefaction beneath the foundations. This mechanism is identified as a primary contributor to observed building settlements.

2.3. Settlement Mechanisms

2.3.1. Settlements due to post-liquefaction compaction

Observed settlements in liquefied areas of Adapazarı (Figure 15; Yoshida et al., 2001) average approximately 10 cm for two- and three-story buildings and exceed 20 cm for four- and five-story buildings. These settlements are smaller than those reported for the 1964 Niigata earthquake, primarily due to the limited thickness of liquefied soil in Adapazarı, which is confined to a layer approximately 2.5 m thick between depths of 1.5 m and 4.0 m.

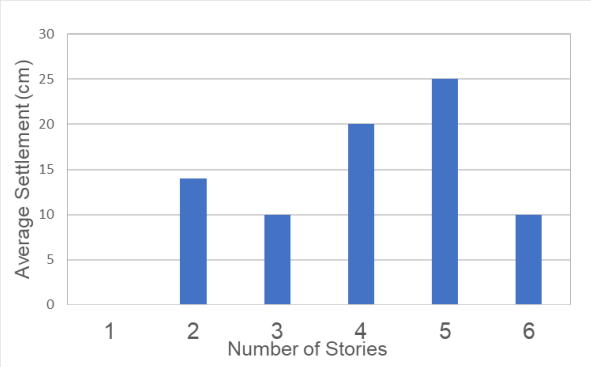

Figure 15. Settlements of the buildings in liquefied area (Yoshida, 2001).

Post-liquefaction volumetric strain depends on initial relative density, maximum shear strain during shaking, and the magnitude of excess pore-water pressure. Tokimatsu and Seed (1987) developed correlations between corrected SPT resistance $(N_1)_{60}$, CSR, and post-liquefaction volumetric strain for earthquakes of magnitude M = 7.5. Integration of these strains over the liquefied layer thickness yields estimated settlements of approximately 7.5–10 cm.

An alternative approach proposed by Ishihara and Yoshimine (1992), based on the factor of safety against liquefaction (CRR/CSR) or maximum cyclic shear strain combined with relative density or penetration resistance, produces comparable settlement estimates.

These values account for only 40–50% of the settlements observed in the field, indicating that additional mechanisms, particularly lateral soil movement beneath foundations, contribute significantly to the total settlement.

2.3.2. Settlements due to lateral slip of supporting soil

Field observations by Richards et al. (1993) demonstrated that seismic settlements of shallow foundations on granular soils are not solely attributable to compaction or liquefaction. Instead, settlements may also result from lateral sliding of the supporting soil beneath foundations once soil strength is exceeded. To model this mechanism, Richards et al. adapted their seismic design approach for retaining walls (Richards and Elms, 1979), which is based on Newmark's (1965) sliding block concept.

Under static conditions, bearing capacity is computed by superposition of soil cohesion, surcharge, and unit weight contributions (equation 18) (Terzaghi, 1943):

$$P_L = cN_c + qN_q + \frac{1}{2}\gamma_s B N_\gamma \tag{18}$$

where c is cohesion, q is surcharge, γ_s is unit weight, and B is foundation width. The bearing capacity factors depend on the internal friction angle ϕ.

The classical Prandtl (1921) bearing capacity mechanism consists of an active wedge, a passive wedge, and an intermediate fan region. For seismic conditions, the fan is eliminated and the mechanism is simplified into active and passive Coulomb wedges. Incorporating inertial forces acting on both the foundation and soil, the seismic capacity (equation 19) becomes (Richards et al., 1993):

$$P_{LE} = cN_{cE} + \gamma_s d N_{qE} + \frac{1}{2}\gamma_s B N_{\gamma E} \tag{19}$$

where N_{cE}, N_{qE}, and $N_{\gamma E}$are seismic bearing capacity factors.

The ratios of seismic to static bearing capacity factors are presented in Figure 16. The results demonstrate that overall foundation capacity deteriorates rapidly with increasing seismic acceleration (Figure 17). As acceleration increases, the size of the failure wedge beneath the foundation decreases, while the active earth pressure coefficient increases and the passive coefficient decreases.

The governing acceleration ratios (equation 20) are:

$$k_h = \frac{a_{h,\max}}{g},\ k_v = \frac{a_{v,\max}}{g} \tag{20}$$

Where $a_{h,\max}$and $a_{v,\max}$are the peak horizontal and

vertical accelerations, respectively, and $g$is gravitational acceleration. The parameters $\rho_{AE}$and ρ_{PE}denote the inclinations of the active and passive wedges relative to the horizontal. A reduction in wedge size implies a smaller force requirement to initiate lateral displacements.

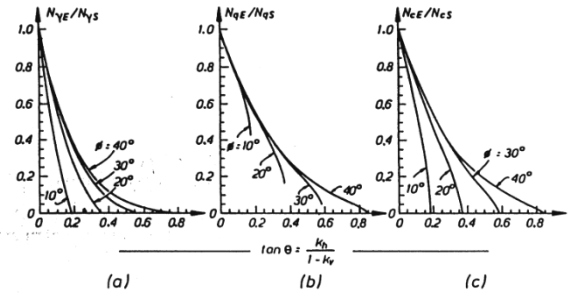

Figure 16. Seismic to static bearing capacity ratios (Richards et al., 1993).

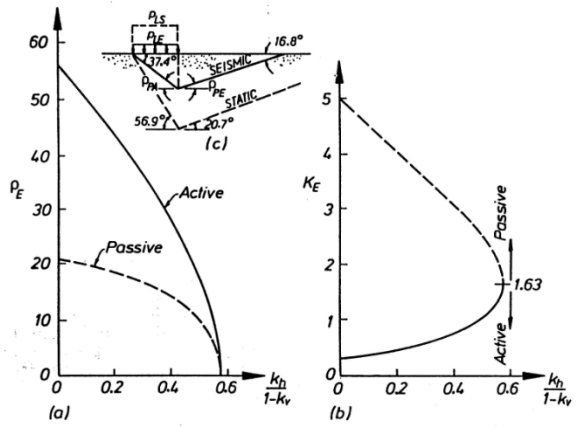

Figure 17. Coulomb wedge analysis for = 30, = /2: (a) Failure surface inclination; (b) seismic pressure coefficients; failure mechanism for (Richards et al., 1993).

Seismic bearing capacity behavior differs fundamentally from static failure. While static bearing failure is associated with large settlements, earthquake-induced bearing settlements occur only when the acceleration ratio exceeds a critical value yield acceleration k_y, $k_h^*/(1-k_v)$, commonly referred to as the cut-off acceleration ratio. For cohesionless soils, this threshold can be expressed as a function of d/B and friction angle ϕ', as illustrated in Figure 18, where d is the depth of the foundation; B is the width of the foundation and ϕ' is internal friction angle of the foundation material.

Once sliding initiates, foundation settlements develop in a manner analogous to the seismic response of retaining walls. The active wedge moves downward, mobilizing passive resistance in accordance with Coulomb theory. Under the sliding block assumption, motion proceeds at constant acceleration until the relative velocity between the moving wedge and stable soil mass reduces to zero. Integration of relative velocity yields displacement along the active slip surface for a given seismic pulse.

3. Results

Sliding block displacements have been evaluated using standardized earthquake records following Newmark (1965). Franklin and Chang (1977) expanded this database, and Richards and Elms (1979) proposed an upper-bound expression (equation 21) for displacement:

$$\Delta = 0.087\frac{V^2}{a_{\max}g}\left(\frac{k_h^*}{a_{\max}}\right)^{-4} \tag{21}$$

where Δ is the unidirectional sliding displacement, $V$is the peak ground velocity, $k_h^*$is the yield acceleration, and $a_{\max}$is the peak horizontal ground acceleration. Because displacements in both directions contribute to settlement, the total settlement (equation 22) is estimated as:

$$w = 2\Delta\tan\rho_{AE} \tag{22}$$

This approach does not explicitly account for time-dependent pore pressure generation. However, once liquefaction occurs, acceleration transfer to upper layers is significantly reduced. Therefore, settlement analyses based on peak ground acceleration without pore pressure effects are considered appropriate.

Although foundation areas typically occupy only one-fourth to one-tenth of the ground area affected, lateral soil displacements beneath foundations can contribute substantially to observed settlements. Consequently, settlements initially attributed solely to liquefaction-induced densification may include a significant component from foundation soil movement.

The two five-story buildings are located along Çırak Street in the Yenigün District, southeast of downtown Adapazarı. Field investigations indicated relatively uniform settlements of approximately 26 cm and 21 cm for the two structures, respectively. The buildings have plan dimensions of approximately 18.3 m by 23 m and are founded on Soil Type 1, as classified by Sancio et al. (2002).

The foundation system consists of a shallow foundation bearing on a 2.5 m thick layer of loose to medium-dense silty sand to sandy silt, underlain by a stratified soil profile comprising 1.5 m of high-plasticity stiff clay, 2.5 m of medium-dense to dense silty fine sand to silt, 2.5 m of clayey silt interbedded with silt and silty sand, and a 5 m thick sequence of silty sand to sandy silt interbedded with silty clay. The groundwater table coincides with the foundation base.

Based on available CPT and SPT data, the friction angle of the soil layer immediately beneath the foundation was estimated as $\phi' = 33°–35°$. Site response analyses yielded a peak ground acceleration of $a_{\max} = 0.3g$and a peak ground velocity of $V = 1.25$m/s. The average foundation pressure was approximately 1 kg/cm^2, and the calculated static factor of safety was about 2.5. With a foundation depth-to-width ratio of 0.08, the corresponding yield acceleration was estimated as $k_h^* \approx 0.18$ (Figure 18).

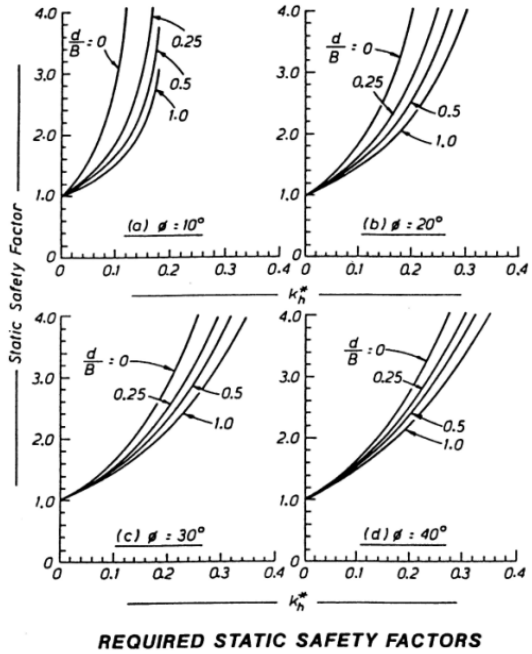

Figure 18. Critical acceleration for incipient foundation settlement (c=0) (Richards et al., 1993).

A schematic representation of incremental settlement caused by the Coulomb sliding wedge mechanism, evaluated using the Newmark (1965) sliding block displacement approach, is presented in Figure 19.

Using $k_h^*/a_{\max} = 0.6$, Equation (21) yields a sliding displacement of $\Delta = 35$cm. With $\rho_{AE} = 0.8$ (Figure 20), Equation (22) results in a total estimated settlement of approximately 56 cm. Of this total, 7.5–10 cm is attributed to liquefaction-induced settlement, while 10–15 cm is associated with lateral movement of foundation soil. The analytical estimate exceeds observed values by a factor of approximately 4–5.

It should be noted that Equation (21) represents an upper-bound relationship derived from a global earthquake database. Given the availability of acceleration time histories from site response analyses, displacements can alternatively be computed for varying yield acceleration levels following the Newmark (1965) sliding block approach.

Accordingly, the TNMN program (Pyke and Beikae, 1991) was employed to perform double integration of acceleration time histories for different yield acceleration values. Figure 5.21 presents the resulting displacements for both directions of motion.

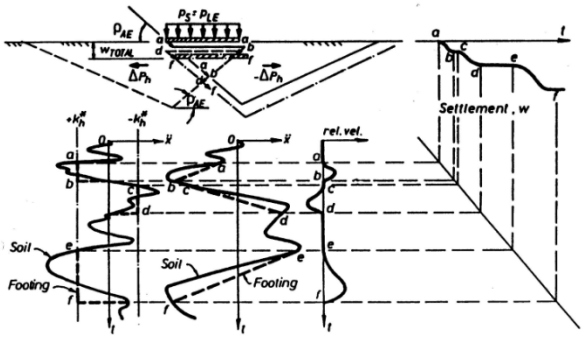

Figure 19. Incremental settlement by Coulomb sliding wedge mechanism (Richards et al., 1993).

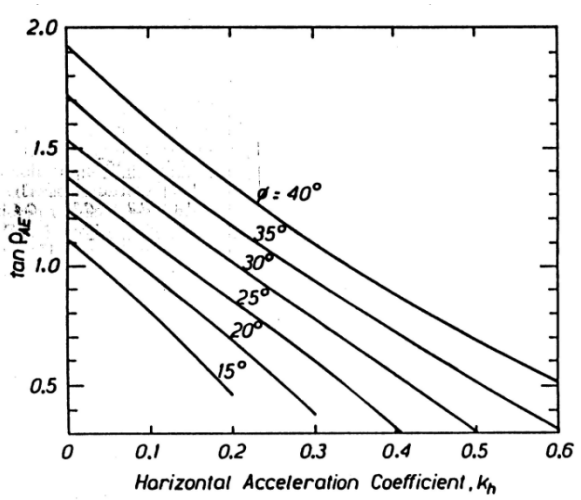

Figure 20. Tangents of active Coulomb wedge angle (Richards et al., 1993).

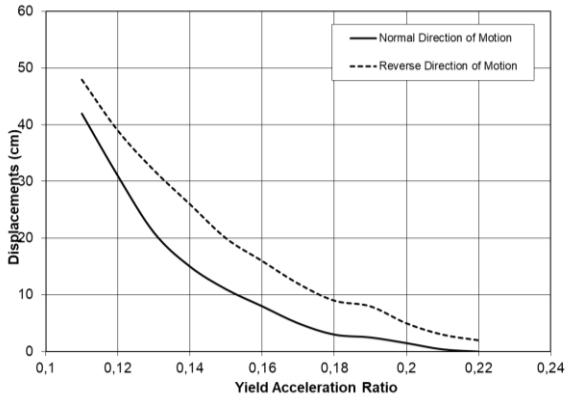

Figure 21. Calculated displacements for different yield acceleration levels.

4. Discussion

The results of this study highlight the complex interaction between ground motion characteristics, soil response, and building behavior in controlling earthquake-induced settlements in deep alluvial basins. Unlike conventional approaches that rely primarily on free-field liquefaction triggering analyses, the findings demonstrate that localized damage patterns in Adapazarı were strongly governed by soil–structure interaction effects and foundation-level deformation mechanisms.

One of the most important outcomes is the discrepancy between simplified free-field liquefaction predictions and observed surface manifestations. Although standard procedures indicated a high liquefaction potential within shallow silty layers, limited free-field evidence of liquefaction cases were documented after the earthquake. This behavior is consistent with previous observations in stiff or partially cemented silty soils, where excess pore pressure generation may be limited by the surrounding stiffer matrix leading to large shear strains or surface ejecta. These results suggest that reliance on simplified penetration-based methods alone may lead to conservative hazard estimates in similar geological environments.

In contrast, the significantly increased cyclic stress ratios underneath the building foundations clearly demonstrate the role of structural inertia and dynamic amplification in modifying subsurface stress conditions. The amplification expected for short-period buildings indicates that resonance between soil and structure can substantially elevate liquefaction susceptibility directly beneath foundations. This finding supports earlier experiences that building-induced stress concentrations can dominate local liquefaction behavior even when free-field conditions remain marginal. Consequently, damage patterns concentrated beneath structures in Adapazarı can be interpreted as a direct consequence of this localized stress amplification.

Settlement analyses further indicate that liquefaction-induced volumetric strain alone cannot fully explain the observed settlements of the buildings. The contribution of foundation sliding associated with seismic bearing-capacity failure provides a physically consistent explanation for the additional settlement component. The agreement between simplified Newmark-type predictions and observed displacements suggests that even relatively simple dynamic sliding models can provide valuable insight when combined with site-specific ground motion estimates. This result emphasizes the importance of considering post-liquefaction strength degradation and inertial loading effects in shallow foundation performance assessments.

From an engineering perspective, the integrated interpretation underscores the limitations of conventional design practices that treat liquefaction triggering and foundation response as independent problems. The interaction between soil nonlinearity, structural response, and foundation-level deformation processes produces coupled effects that strongly influence damage distribution. The Adapazarı case study demonstrates that settlement estimates may be undervalued if free-field analyses are used as the sole basis for performance evaluation in urban environments.

Despite the valuable insights provided, several limitations should be acknowledged. Uncertainties remain in the estimation of site-specific soil properties, post-liquefaction strength parameters, and nonlinear damping characteristics. In addition, the use of one-dimensional site response analyses does not fully capture potential three-dimensional basin effects and lateral heterogeneity. Future studies incorporating two- or three-dimensional numerical modeling, better geotechnical data, and detailed building inventory information would further improve the accuracy of settlement predictions.

Overall, the findings reinforce the need for performance-based seismic assessment frameworks that explicitly incorporate soil–structure interaction and foundation deformation mechanisms. Such approaches are particularly critical for heavily built urban areas located on deep alluvial deposits, where conventional liquefaction evaluation methods may fail to capture the true causes of earthquake-induced damage.

5. Conclusions

This study investigated the ground motion characteristics, liquefaction potential, and building settlement mechanisms in downtown Adapazarı during the 17 August 1999 Kocaeli earthquake, with particular emphasis on the interaction between soil response and building behavior. The main conclusions are summarized as follows:

- Nonlinear site response analyses calibrated with recorded aftershocks indicate that the peak ground acceleration in downtown Adapazarı was approximately 0.30 g, consistent with empirical relationships for deep alluvial basins and suitable for liquefaction and settlement evaluation.
- Simplified free-field liquefaction analyses predict triggering within shallow silty and sandy silt layers (1.5–4.0 m depth); however, the absence of clear surface manifestations suggests that conventional simplified procedures are conservative for the local soil conditions.
- The relatively stiff soil matrix limited cyclic shear strain development in free-field conditions, reducing the extent of observable liquefaction effects.
- Cyclic stress ratios beneath buildings were significantly higher than free-field values due to structural inertia and dynamic amplification, particularly for short-period structures (0.3–0.6 s), increasing liquefaction susceptibility beneath foundations.
- Soil–structure interaction effects were identified as a primary factor governing localized liquefaction response and damage concentration beneath buildings.
- Liquefaction-induced volumetric strains account for approximately 40–50% of the observed building settlements, while the remaining settlements are primarily attributed to lateral foundation sliding associated with exceedance of seismic bearing capacity.
- Simplified Newmark-type sliding block analyses

using site-specific acceleration time histories produced settlement estimates consistent with field observations.

- The observed settlement patterns cannot be explained by free-field liquefaction alone but instead result from the combined effects of suppressed free-field liquefaction, amplified cyclic stresses beneath structures, and lateral soil movement due to foundation sliding.
- Conventional free-field liquefaction assessments are therefore insufficient for predicting structural performance in urban areas underlain by shallow, heterogeneous, and highly deformable soils.
- Incorporating simplified soil–structure interaction and seismic bearing-capacity considerations significantly improves post-earthquake damage interpretation and settlement prediction.

When evaluating liquefaction risks and earthquake-induced settlements in deep alluvial basins, this work emphasizes the significance of incorporating nonlinear site response analysis, building response effects, and foundation-level deformation mechanisms. The findings offer useful information for post-quake assessments and for enhancing seismic design and assessment techniques for structures with shallow foundations in comparable geological environments.

Author Contributions

The percentages of the author' contributions are presented below. The author reviewed and approved the final version of the manuscript.

	D.Y.
C	100
D	100
S	100
DCP	100
DAI	100
L	100
W	100
CR	100
SR	100
PM	100
FA	100

C= concept, D= design, S= supervision, DCP= data collection and/or processing, DAI= data analysis and/or interpretation, L= literature search, W= writing, CR= critical review, SR= submission and revision, PM= project management, FA= funding acquisition.

Conflict of Interest

The author declared that there is no conflict of interest.

Ethical Consideration

Ethics committee approval was not required for this study because of there was no study on animals or humans.

References

Bard, P.-Y., & Bouchon, M. (1985). The two-dimensional resonance of sediment-filled valleys. *Bulletin of the Seismological Society of America*, *75*(2), 519–541.

Boulanger, R. W. (2003). Relating cyclic resistance of sands to relative state parameter index. *Journal of Geotechnical and Geoenvironmental Engineering*, *129*(8), 770–773.

Bray, J. D., & Rathje, E. R. (1998). Earthquake-induced displacements of solid-waste landfills. *Journal of Geotechnical and Geoenvironmental Engineering*, *124*(3), 242–253.

Bray, J. D., Sancio, R. B., Youd, T. L., Christensen, C., Çetin, O., Önalp, A., Durgunoğlu, H. T., Stewart, J. P., Seed, R. B., Baturay, M. B., Karadayılar, T., & Emrem, C. (2001). *Documenting incidents of ground failure resulting from the August 17, 1999 Kocaeli, Turkey earthquake* (PEER Report). University of California, Berkeley.

Chang, S. W., Bray, J. D., & Gookin, W. (1997). *Seismic response of deep stiff soil deposits in the Los Angeles area during the 1994 Northridge earthquake* (Geotechnical Engineering Report UCB/GT-97-01). University of California, Berkeley.

Durgunoğlu, H. T., Karadayılar, T., Bray, J. D., Sancio, R. B., & Hacıalioğlu, E. (2000). *Geotechnical–geodynamic profiling by seismic CPT*. 8th National Congress on Soil Mechanics and Foundation Engineering, Istanbul (in Turkish).

EERI (2000). *The İzmit (Turkey) earthquake of August 17, 1999: Reconnaissance report*. Earthquake Engineering Research Institute.

Franklin, A. G., & Chang, F. K. (1977). *Permanent displacements of earth embankments by Newmark sliding block analysis* (Report S-71). U.S. Army Waterways Experiment Station.

Hashash, Y. M. A., & Park, D. (2001). Nonlinear one-dimensional seismic ground motion propagation. *Engineering Geology*, *62*(1-3), 1–20.

Hudson, M., I. M. Idriss, and M. Beikae, (1994). QUAD4M A Computer Program to Evaluate the Seismic Response of Soil Structures Using Finite Element Procedures and Incorporating a Compliant Base, Center for Geotechnical Modeling Department of Civil and Environmental Engineering, University of California, Davis, California.

Idriss, I. M. (1991). Earthquake ground motions at soft soil sites. *In Proceedings of the 2nd International Conference on Recent Advances in Geotechnical Earthquake Engineering and Soil Dynamics* (Vol. 3, pp. 2265–2271). University of Missouri-Rolla.

Ishihara, K. (1993). Liquefaction and flow failure during earthquakes. *Géotechnique*, *43*(3), 351–415.

Ishihara, K., & Yoshimine, P. (1992). Evaluation of settlements in sand deposits following liquefaction during earthquakes. *Soils and Foundations*, *32*(1), 173–188.

Joyner, W. B. and A. T. F. Chen, (1975). "Calculation of non-linear ground response in earthquakes." Bulletin of Seismological Society of America, Vol. 65, pp. 1315-1336.

Komazawa, M., Morikawa, H., Nakamura, K., Akamatsu, J., Nishimura, K., Sawada, S., Erken, A., & Önalp, A. (2002). Bedrock structure in Adapazarı as a possible cause of severe damage during the 1999 Kocaeli earthquake. *Soil Dynamics and Earthquake Engineering*, *22*(9-12), 829–836.

Kramer, S. L. (1996). *Geotechnical earthquake engineering*. Prentice Hall.

Marcuson, W. F., III. (1978). Definition of terms related to liquefaction. *Journal of the Geotechnical Engineering Division*, *104*(9), 1197–1200.

Matasovic, N. (1993). *Seismic response of composite horizontally layered soil deposits* [Doctoral dissertation]. University of California, Los Angeles.

Newmark, N. M. (1965). Effects of earthquakes on dams and embankments. *Géotechnique*, *15*(2), 139–160.

Newmark, N. M., & Hall, W. J. (1982). *Earthquake spectra and design*. Earthquake Engineering Research Institute.

National Research Council (NRC). 1985. Liquefaction of Soils During Earthquakes. Committee on Earthquake Engineering, Commission on Engineering and Technical Systems, National Research Council, National Academy Press, Washington, DC, 255 pages. DOI:10.17226/19275.

Prandtl, L. (1921). "Uber die eindringungstestigkeit plastisher baustoffe un die festigkeit von schneiden." Zeitschrift Für Angewandt Mathematik Und Mechanik, 1(1), pp. 15-30 (in German). As referenced by Richards et al. 1993.

Pyke, R. (2003). Liquefaction resistance of soils: Summary report from NCEER workshops. *Journal of Geotechnical and Geoenvironmental Engineering*, *127*(10), 817–833.

Pyke, R. (2004). *Consulting report for Demirözü Dam*.

Pyke, R., & Beikae, M. (1991). *TNMN*. Taga Engineering Software Services.

Rial, J. A., Saltzman, N. G., & Ling, H. (1992). Earthquake-induced resonance in sedimentary basins. *American Scientist*, *80*(6), 566–578.

Richards, R., & Elms, D. G. (1979). Seismic behavior of gravity retaining walls. *Journal of the Geotechnical Engineering Division*, *105*(4), 449–464.

Richards, R., Elms, D. G., & Budhu, M. (1993). Bearing capacity and settlements of foundations. *Journal of Geotechnical Engineering*, *119*(4), 662–674.

Rollins, K. M., & Seed, H. B. (1990). Influence of buildings on potential liquefaction damage. *Journal of Geotechnical Engineering*, *116*(2), 165–185.

Rosenblad, B., E. M. Rathje and K. H. Stokoe, Shear Wave Velocity Profiling by the SASW Method at Selected Strong-Motion Stations in Turkey, Report published by University of Texas at Austin, Texas, 2003.

Sancio, R. B., Bray, J. D., Stewart, J. P., Youd, T. L., Durgunoğlu, H. T., Önalp, A., Seed, R. B., Christensen, C., Baturay, M. B., & Karadayılar, T. (2002). Correlation between ground failure and soil conditions in Adapazarı. *Soil Dynamics and Earthquake Engineering*, *22*(9-12), 1093–1102.

Schnabel, P. B., Lysmer, J., & Seed, H. B. (1972). *SHAKE: A computer program for earthquake response analysis of horizontally layered sites* (Report No. EERC 72-12). Earthquake Engineering Research Center, University of California, Berkeley.

Seed, H. B. (1979). Soil liquefaction and cyclic mobility evaluation for level ground during earthquakes. *Journal of the Geotechnical Engineering Division*, *105*(2), 201–255.

Seed, H. B., & Idriss, I. M. (1971). Simplified procedure for evaluating soil liquefaction potential. *Journal of the Soil Mechanics and Foundations Division*, *97*(9), 1249–1273.

Seed, H. B., & Idriss, I. M. (1982). *Ground motions and soil liquefaction during earthquakes*. Earthquake Engineering Research Institute Monograph.

Seed, H. B., Tokimatsu, K., Harder, L. F., & Chung, R. M. (1985). The influence of SPT procedures in soil liquefaction resistance evaluations. *Journal of Geotechnical Engineering*, *111*(12), 1425–1445.

Terzaghi, K., Theoretical soil mechanics, John Wiley & Sons, Inc., New York, 1943.

Tokimatsu, K., & Seed, H. B. (1987). Evaluation of settlements in sands due to earthquake shaking. *Journal of Geotechnical Engineering*, *113*(8), 861–878.

Yilmaz, D. (2003). *Site response and settlement of buildings in Adapazari basin* [Doctoral dissertation]. Bogazici University.

Youd, T. L., & Idriss, I. M. (Eds.). (1997). *Proceedings, NCEER Workshop on Evaluation of Liquefaction Resistance of Soils*. National Center for Earthquake Engineering Research, State University of New York at Buffalo.

Youd, T. L., & Idriss, I. M. (2001). Liquefaction resistance of soils: Summary report from NCEER/NSF workshops. *Journal of Geotechnical and Geoenvironmental Engineering*, *127*(4), 297–313.

Yoshida, N., Tokimatsu, K., Yasuda, S., Kokusho, T., & Okimura, T. (2001). Geotechnical aspects of damage in Adapazarı during the 1999 Kocaeli earthquake. *Soils and Foundations*, *41*(4), 25–45.